

Spin-Lattice Coupling and Frustrated Magnetism in Fe-doped Hexagonal LuMnO₃

Harikrishnan S. Nair,^{1,*} Zhendong Fu,² C. M. N. Kumar,^{3,4} V. Y. Pomjakushin,⁵ Yinguo Xiao,⁶ Tapan Chatterji,⁷ and André M. Strydom^{1,8}

¹Highly Correlated Matter Research Group, Physics Department,
P. O. Box 524, University of Johannesburg, Auckland Park 2006, South Africa

²Jülich Center for Neutron Sciences JCNS, Outstation at MLZ,
Forschungszentrum Jülich GmbH, Lichtenberg Straße 1, D-52474 Garching, München, Germany

³Jülich Centre for Neutron Science JCNS, Outstation at SNS,
Oak Ridge National Laboratory, Oak Ridge, Tennessee 37831, United States

⁴Chemical and Engineering Materials Division, Oak Ridge National Laboratory, Oak Ridge, Tennessee 37831, United States

⁵Laboratory for Neutron Scattering, Paul Scherrer Institute, CH-5232 Villigen, Switzerland

⁶Jülich Center for Neutron Sciences JCNS and Peter Grünberg Institute PGI,
JARA-FIT, Forschungszentrum Jülich GmbH, 52425 Jülich, Germany

⁷Institut Laue-Langevin, BP 156, 38042 Grenoble Cedex 9, France

⁸Max Planck Institute for Chemical Physics of Solids, Nöthnitzerstraße 40, 01187 Dresden, Germany

(Dated: October 17, 2018)

Strong spin-lattice coupling and prominent frustration effects observed in the 50% Fe-doped frustrated hexagonal (*h*)LuMnO₃ are reported. A Néel transition at $T_N \approx 112$ K and a possible spin re-orientation transition at $T_{SR} \approx 55$ K are observed in the magnetization data. From neutron powder diffraction data, the nuclear structure at and below 300 K was refined in polar $P6_3cm$ space group. While the magnetic structure of LuMnO₃ belongs to the Γ_4 ($P6_3c'm$) representation, that of LuFe_{0.5}Mn_{0.5}O₃ belongs to Γ_1 ($P6_3cm$) which is supported by the strong intensity for the (100) reflection and also judging by the presence of spin-lattice coupling. The refined atomic positions for Lu and Mn/Fe indicate significant atomic displacements at T_N and T_{SR} which confirms strong spin-lattice coupling. Our results complement the discovery of room temperature multiferroicity in thin films of *h*LuFeO₃ and would give impetus to study LuFe_{1-x}Mn_xO₃ systems as potential multiferroics where electric polarization is linked to giant atomic displacements.

PACS numbers:

Hexagonal manganites (*h*)RMnO₃ (*R* = rare earth) are fascinating systems in the class of multifunctional oxides which present multiferroicity[1–3], dielectric and magnetic anomalies,[4] field-induced re-entrant phases,[5] metamagnetic steps in magnetization[6] and recently, even found related to cosmology[7]. The primary interest in hexagonal manganites arises from the potential to realize multiferroics since it was found that below the ferroelectric transition temperature, $T_{FE} \approx 1000$ K, they develop electric polarization due to structural distortions and giant atomic displacements[2, 3]. *h*RMnO₃ systems often have a low Néel temperature T_N (often ≤ 100 K) compared to the T_{FE} . Strong coupling between lattice, magnetic and electric degrees of freedom is generally observed in hexagonal manganites despite the large separation in temperature between T_{FE} and T_N [8]. The magnetic structure of *h*RMnO₃ presents significant complexity in the form of magnetic frustration where the Mn moments in *ab*-plane form 120° triangular lattice[9]. This 2D edge-sharing triangular network is geometrically frustrated with antiferromagnetic nearest-neighbor exchange interaction and gives rise to diffuse magnetic scattering intensity close to T_N [10].

There exist significantly many reports on the magnetic structure of hexagonal manganites in different representations due to the homometric pairs of irreducible representations

that yield the same neutron diffraction pattern if the x (Mn) is the ideal value of ($\frac{1}{3}$). One of the most-studied hexagonal manganite, YMnO₃ has been reported in several symmetries by different authors – Γ_3 [11], Γ_1 [12] or Γ_5 , Γ_6 [9]. Earlier investigations suggested Γ_1 or Γ_3 as the possible magnetic structure for YMnO₃[13]. However, neutron polarimetry studies have confirmed the magnetic structure as Γ_5 or Γ_6 [9]. On the other hand, *h*LuMnO₃ which shares most of the properties of *h*YMnO₃ has Γ_4 ($P6_3c'm$) symmetry[10, 14]. In both *h*YMnO₃ and *h*LuMnO₃, strong spin-lattice coupling triggered by giant atomic displacements of Mn ion at T_N plays an important role in inducing ferroelectric distortion leading subsequently to multiferroic property.

Compared to *h*LuMnO₃, the ferrite *h*LuFeO₃ is reported to present improved magnetic properties[15]. In a recent study on *h*LuFeO₃, strong exchange coupling leading to high magnetic transition temperatures and spin re-orientation transitions closely connected with structural distortions have been identified[16]. Thin films of *h*LuFeO₃ have shown evidence for a room temperature multiferroic[17] and has been identified as a strong candidate for linear magneto-electric coupling and control of the ferromagnetic moment directly by an electric field[18]. However, bulk LuFeO₃ normally crystallizes in orthorhombic *Pbnm* symmetry thereby precluding the possibility of ferroelectricity. Hence it is desirable to prepare solid solutions of *h*RMnO₃ and *h*RFeO₃ in order to combine the features of giant atomic displacements that lead to ferroelectric polarization and the magnetic transitions at near-300 K. In the present work, the

*Electronic address: h.nair.kris@gmail.com, hsnair@uj.ac.za

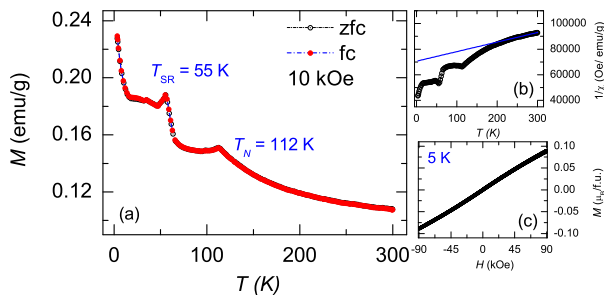


FIG. 1: (colour online) (a) Magnetization curves of $\text{LuFe}_{0.5}\text{Mn}_{0.5}\text{O}_3$ in zero field-cooled (zfc) and field-cooled (fc) modes at an applied field of 10 kOe. Two magnetic transitions occur at $T_N \approx 112$ K and $T_{\text{SR}} \approx 55$ K. (b) Presents the inverse susceptibility suggesting presence of spin fluctuations at $T \geq T_N$. The solid line is Curie-Weiss fit. (c) Shows field-scans of magnetization at 5 K.

solid solution $\text{LuFe}_{0.5}\text{Mn}_{0.5}\text{O}_3$ has been synthesized and is studied using magnetization and neutron powder diffraction. The results reveal strong spin-lattice coupling in this material and suggest its potential to be a multiferroic.

The polycrystalline samples used in the present study were prepared by following a solid state reaction method[4]. High purity Lu_2O_3 , Fe_2O_3 and MnO (4N, Sigma Aldrich) were used as the precursors. The synthesized powder sample was first characterized using laboratory x rays. Formation of a single hexagonal phase without impurities was confirmed in this way. Magnetic measurements were performed using a Magnetic Property Measurement System, Quantum Design Inc. Neutron powder diffraction experiments were carried out at the SINQ spallation source of Paul Scherrer Institute (Switzerland) using the high-resolution diffractometer for thermal neutrons HRPT[19] with the wavelength $\lambda = 1.886$ Å in high intensity mode. About 8 g of powder sample was used to obtain the neutron powder patterns which were recorded at 11 temperature points between 2 K and 300 K. The nuclear and magnetic structure refinements were performed using Rietveld method[20] employing FULLPROF code[21]. Magnetic structure refinement using representation analysis was performed using the software SARA h [22].

Magnetization measurements in zero field-cooled (zfc) and field-cooled (fc) protocols recorded for $\text{LuFe}_{0.5}\text{Mn}_{0.5}\text{O}_3$ are presented in Fig 1 (a) for 10 kOe. Two magnetic phase transitions are identified at $T_N \approx 112$ K and $T_{\text{SR}} \approx 55$ K. At T_N , the Néel transition in the 120° triangular lattice takes place. In the case of $h\text{LuMnO}_3$ a lower value of $T_N \approx 88$ K was observed. The transition at T_{SR} in $\text{LuFe}_{0.5}\text{Mn}_{0.5}\text{O}_3$ could be a spin re-orientation transition similar to the one found in $h\text{LuFeO}_3$ at 130 K[16]. The T_{SR} in $h\text{LuFeO}_3$ is closely related to the interlayer exchange coupling and the atomic displacements due to the K_1 phonon mode[16]. The frustration effects in $\text{LuFe}_{0.5}\text{Mn}_{0.5}\text{O}_3$ are clearly seen in the inverse magnetic susceptibility $1/\chi(T)$ which shows deviation from linear trend even for $T \gg T_N$, as seen from the Curie-Weiss fit in (b). From the Curie-Weiss fit, an effective paramagnetic moment value, $\mu_{\text{eff}} = 5.41(4) \mu_B$ and Curie-Weiss temperature, $\Theta_{\text{CW}} = -946$ K are estimated.

The effective paramagnetic moment calculated assuming spin-only contributions is $\mu_{\text{calc}} = 5.4 \mu_B$. As an estimate of frustration, the ratio $f = |\Theta_{\text{CW}}|/T_N \approx 8.5$ is calculated. This value of f signals significant frustration effects and is comparable to the frustration indices of other hexagonal systems collected in Table I. A field-scan performed in zero field-cooled protocol at 5 K is presented in Fig 1 (c) where no hysteresis is observed. There is no indication of ferromagnetic contribution to magnetic susceptibility. The maximum magnetic moment obtained at 5 K under 90 kOe ($\approx 0.1 \mu_B/\text{f.u.}$) is significantly reduced in magnitude compared to the value for the ferromagnetic alignment of Mn^{3+} and Fe^{3+} moments; $5.4 \mu_B/\text{f.u.}$. The antiferromagnetic arrangement of moments in the basal plane and the resulting strong frustration effects leads to this reduction in observed magnetic moment. In addition to the purely geometrical frustration effects, low dimensionality of the hexagonal plane brought about by the competition between the intra-plane and the inter-plane exchange interactions, also plays a role in the separation between T_N and Θ_{CW} .

The experimentally obtained neutron powder diffraction pattern for $\text{LuFe}_{0.5}\text{Mn}_{0.5}\text{O}_3$ at 300 K and 2 K are presented in Fig 2 (a) and (b) respectively. The calculated patterns refined using the Rietveld method are also shown. It is known that the hexagonal manganites undergo a phase transition from centrosymmetric $P6_3/mmc$ to ferroelectric $P6_3cm$ below $T_{\text{FE}} \approx 1000$ K[3]. It is found that the nuclear structure of $\text{LuFe}_{0.5}\text{Mn}_{0.5}\text{O}_3$ remains $P6_3cm$ in the temperature range 300 - 2 K. The refined lattice parameters and the atomic coordinates for 300 K and 2 K are presented in Table II. The refined Mn position at 10 K is $x = 0.334$. For a perfect 2D triangular network, the ideal value is $x = \frac{1}{3}$ and it is reported to be 0.340 for $h\text{YMnO}_3$ and 0.331 for $h\text{LuMnO}_3$ [24]. The displacements of the Mn atom as suggested by the x position have strong correlation with the magnetic structure. The Mn-Mn interactions between adjacent Mn planes are due to superexchange mechanism via the apical oxygens of MnO_5 bipyramids. When $x = (\frac{1}{3})$, all exchange paths are equivalent. However, when $x \neq (\frac{1}{3})$, two different paths with two different exchange interactions, J_{z1} and J_{z2} , are formed. Thus $x = (\frac{1}{3})$ is a critical threshold value and determines the stability of magnetic structure below T_N [12, 15].

Below $T_N \approx 112$ K, a purely magnetic reflection is observed at (101) at $2\Theta \approx 23^\circ$ ($d_{hkl} = 4.72$ Å) and enhancement of nuclear intensity at (102) at $2\Theta \approx 28^\circ$ ($d_{hkl} = 3.85$ Å; see Fig 2 (b), inset) suggesting antiferromagnetic ordering in the triangular lattice with Mn/Fe moments aligned 120° to each other. The magnetic structure of $\text{LuFe}_{0.5}\text{Mn}_{0.5}\text{O}_3$ below T_N was solved by assuming $\mathbf{k} = (0, 0, 0)$ propagation vector for the nuclear space group $P6_3cm$. Representation analysis for magnetic structure then allows six possible solutions: $\Gamma_1 (P6_3cm)$, $\Gamma_2 (P6_3c'm')$, $\Gamma_3 (P6_3c'm')$, $\Gamma_4 (P6_3c'm')$, $\Gamma_5 (P6_3)$ and $\Gamma_6 (P6_3')$ [9, 14]. The magnetic structure of $h\text{LuMnO}_3$ belongs to the representation $\Gamma_4 (P6_3c'm')$ [10, 14]. However, non-zero intensity for the (100) reflection which is stronger compared to the (101) could suggest that the $\Gamma_3 (P6_3c'm')$ or $\Gamma_1 (P6_3cm)$ models are the correct one for the Fe-doped compound. The 2 K

TABLE I: The Curie-Weiss temperature, Θ_{CW} , the Néel temperature, T_N and the frustration parameter, f of some of the highly frustrated hexagonal manganites. The values for $\text{LuFe}_{0.5}\text{Mn}_{0.5}\text{O}_3$ closely compare with those for other related hexagonal systems.

Compound	Θ_{CW} (K)	T_N (K)	f	Ref.
YMnO_3	-545	75	7.8	[23]
LuMnO_3	-740	≈ 90	≈ 8	[24]
$(\text{Y,Lu})\text{MnO}_3$	-600 to -800	≈ 70 to 90	≈ 8	[24]
Lu(Fe,Mn)O_3	-946	112	8.5	[This Work]

TABLE II: The refined lattice parameters and atomic positions of $\text{LuFe}_{0.5}\text{Mn}_{0.5}\text{O}_3$ at 300 K and 2 K. The refinement was carried out using the nuclear space group $P6_3cm$ (#185). The atomic positions are: Lu1 $2a$ (0,0, z); Lu2 $4b$ ($\frac{1}{3}, \frac{2}{3}, z$); Fe/Mn $6c$ ($x, 0, z$); O1 $6c$ ($x, 0, z$); O2 $6c$ ($x, 0, z$); O3 $2a$ (0,0, z); O4 $4b$ ($\frac{1}{3}, \frac{2}{3}, 0$). The isotropic thermal parameters were fixed at the values obtained from [13].

	300 K	2 K
a (Å)	6.0094(5)	5.9962(9)
c (Å)	11.5440(24)	11.5415(31)
Lu1: z	0.213(46)	0.090(51)
Lu2: z	0.172(33)	0.049(12)
Fe/Mn: x	0.348(117)	0.335(28)
z	-0.057(57)	-0.179(22)
O1: x	0.308(23)	0.308(18)
z	0.072(32)	0.072(12)
O2: x	0.640(28)	0.640(25)
z	0.242(34)	0.242(23)
O3: z	0.373(37)	0.373(22)
O4: z	-0.078(45)	-0.078(24)

data with the Rietveld refinement fits assuming Γ_1 model is presented in Fig 2 (b). The indices of low-angle nuclear and magnetic reflections are marked in the figure. A part of the diffraction data is magnified in the inset of (b) to show the magnetic peaks and the fits. A comparison of the diffraction patterns obtained at 75 K and 100 K which lie between the T_N and the T_{SR} is presented in the panel (c). The reflections at (100) and (102) are seen to undergo an enhancement in intensity with the reduction in temperature. This could be an indication of the progressive change in the magnetic structure below the T_N . The magnetic refinement above the T_{SR} was performed using the Γ_1 ($P6_3cm$) and the Γ_3 ($P6_3cm'$) representations and was found that they both gave equivalent description of the observed data. Analysis was also carried out using the representation Γ_2 ($P6_3cm'$) however, it could not reproduce the experimental magnetic intensities faithfully. Within the present set of measurements, it is not possible to clearly confirm a spin re-orientation at T_{SR} in this compound. In Fig 2 (d) a comparison of the 2 K data of $h\text{LuMnO}_3$ and $\text{LuFe}_{0.5}\text{Mn}_{0.5}\text{O}_3$ is presented. Note that the (100) peak is absent in the $h\text{LuMnO}_3$ data.

Trimerization instability,[2, 24] single ion anisotropy and Dzyaloshinskii-Moriya interactions are anticipated for the $P6_3cm$ structure and could play a role in determining the magnetic ground state. The details of how all these factors lead to a complex magnetic structure is yet to be understood. It was noted in the work by Solovyev *et al.*,[14] using first-principles methods that the different magnetic ground state models for $h\text{YMnO}_3$ and $h\text{LuMnO}_3$ have close-by energies. In doped compounds of $h\text{YMnO}_3$ and $h\text{LuMnO}_3$, refinement using combination of different representations

have been used to get a better result[24, 25].

In Fig 3 (a) (b) and (c), the refined atomic positions, x of Mn/Fe and z of Lu1 and Lu2 are plotted as a function of temperature. The atomic displacements are significantly large and comparable to the giant atomic displacements found in $h\text{YMnO}_3$ [2]. Especially, the x position deviates from the ideal value of $\frac{1}{3}$ for ideal 2D triangular network. Note that (a) presents an anomaly at T_{SR} and suggest strong spin-lattice coupling. Huge atomic displacements of all the atoms in the unit cell were found to occur below T_N in multiferroic $h(\text{Y/Lu})\text{MnO}_3$ leading to strong spin-lattice coupling[2]. The relative shift in Mn x amounts to about 4 % which is comparable to the values found for $h\text{YMnO}_3$ [2] or for Ti displacements in a conventional ferroelectric like BaTiO_3 [26]. It is interesting to note that the variation of Mn x in YMnO_3 and LuMnO_3 are in opposite directions, meaning, in one case the x value increases from the ideal x value where as in the other, it decreases. In the case of $\text{LuFe}_{0.5}\text{Mn}_{0.5}\text{O}_3$, the Mn x variation resembles closely that of YMnO_3 [2]. In (d), the temperature-evolution of magnetic moment is presented which shows a continuous reduction in magnetic moment and confirms a phase transition at T_N , however, at T_{SR} no anomaly is present. The ordered magnetic moment in $\text{LuFe}_{0.5}\text{Mn}_{0.5}\text{O}_3$ at 2 K estimated from the neutron diffraction data is $3.3 \mu_B/\text{f.u.}$ which is comparable to the theoretical value of $3 \mu_B$ for $h\text{LuMnO}_3$ [10].

From the magnetization data on $\text{LuFe}_{0.5}\text{Mn}_{0.5}\text{O}_3$, it is clear that two magnetic transitions take place in this hexagonal manganite, at ≈ 112 K and ≈ 55 K. The transition at 112 K is confirmed as a paramagnetic-to-antiferromagnetic phase transition. The neutron diffraction data confirms the

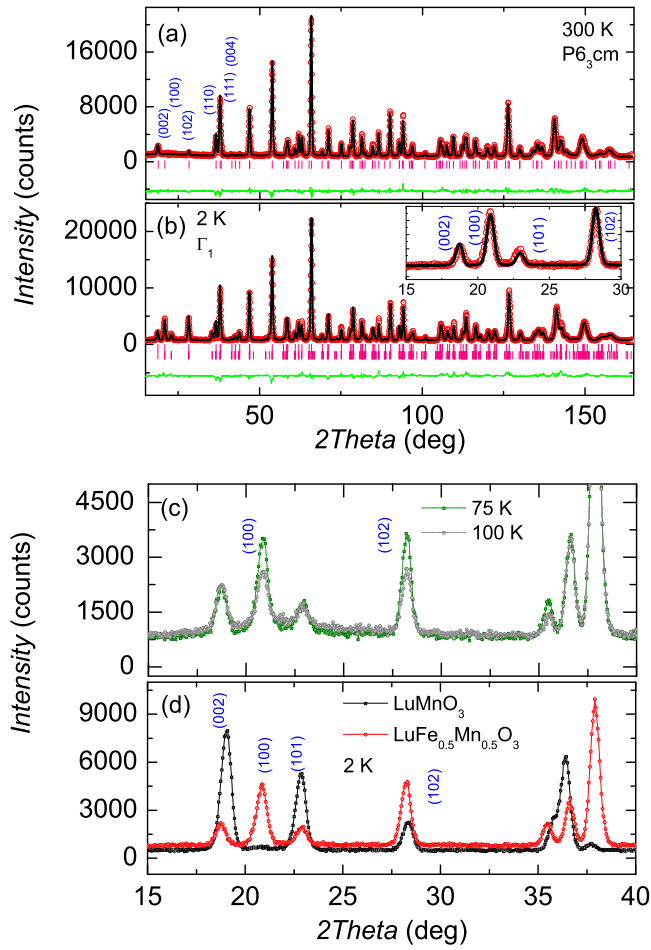


FIG. 2: (colour online) The neutron powder diffraction data on $\text{LuFe}_{0.5}\text{Mn}_{0.5}\text{O}_3$ along with Rietveld refinement for (a) 300 K and (b) 2 K. The nuclear structure is refined in $P6_3cm$ space group. In (b), the magnetic structure is modeled after Γ_1 . The calculated pattern is plotted as a black line and the difference plot as a green line. The Bragg positions are marked as pink vertical bars. In (b), the bottom row of ticks represent magnetic peaks. The inset of (b) magnifies the low-angle reflections, especially the (100), which is typically strong for Γ_1 . (c) Shows the plot comparing the patterns at 75 K and 100 K which highlight an enhancement of intensity for the reflections (100) and (102). (d) Shows a comparison of the 2 K data of $h\text{LuMnO}_3$ and $\text{LuFe}_{0.5}\text{Mn}_{0.5}\text{O}_3$ to contrast Γ_1 (Γ_3) and Γ_2 (Γ_4).

room temperature nuclear structure as $P6_3cm$. Further, the 2 K data is analyzed faithfully using two magnetic representations - the Γ_1 ($P6_3cm$) and Γ_3 ($P6'_3cm'$). The presence of strong intensity for (100) reflection rules out the Γ_2 ($P6_3c'm'$) and Γ_4 ($P6'_3c'm$) models. Both the models Γ_1 and Γ_3 gave reasonable and comparable reliability factors of refinement. However, a reasonable value for the Mn/Fe x position was obtained only with the Γ_1 model. For the other model, the refined x -value was largely off from the ideal value of $\frac{1}{3}$. In addition, magneto-electric coupling in hexagonal manganites is only allowed for magnetic structures where the six-fold symmetry axis is not combined with

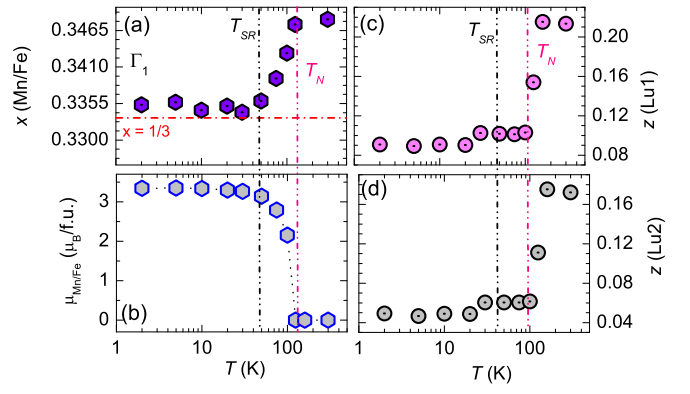


FIG. 3: (colour online) The refined atomic positions, x for Mn/Fe and z for Lu1 and Lu2 are shown in (a), (b) and (c) respectively. The horizontal line in (a) corresponds to the ideal value of $x = \frac{1}{3}$ for ideal 2D triangular network. All the three show an anomalous change at T_{SR} indicating strong spin-lattice coupling. The T_{SR} and the T_N are marked as black dash-dotted lines. (d) Shows the variation of ordered magnetic moment as a function of temperature. Error bars were typically of the size of the data point.

time reversal symmetry[9]. This excludes Γ_3 ($P6'_3cm'$), Γ_4 ($P6_3c'm$) and Γ_6 ($P6'_3$) structures[9]. Hence it can be concluded from the observation of significant atomic displacements in the magnetic phase, that the magnetic structure of $\text{LuFe}_{0.5}\text{Mn}_{0.5}\text{O}_3$ must be Γ_1 below 112 K. In a recent report, Disseler *et al.*, studied the magnetic structure of $\text{LuFe}_{0.75}\text{Mn}_{0.25}\text{O}_3$ [28]. They observed a $T_N \approx 134$ K and the presence of scattering intensity at (100) and (101) reflections above the T_N suggesting that correlations related to both Γ_1 and Γ_2 were present. First-principles calculations on hexagonal ferrites and manganites[15] do indicate that the energy of Γ_1 and Γ_2 are close and are separated by an amount smaller than the single ion anisotropy.

Though giant displacements of the atomic positions of Mn and Lu are observed at T_{SR} , such an anomaly is not reflected in the temperature variation of magnetic moment. Hence, it is not possible to confirm a possible change of magnetic structure between Γ_1 and Γ_3 at or below 55 K. Detailed studies employing single crystals of this composition is required to settle that question. The important result of

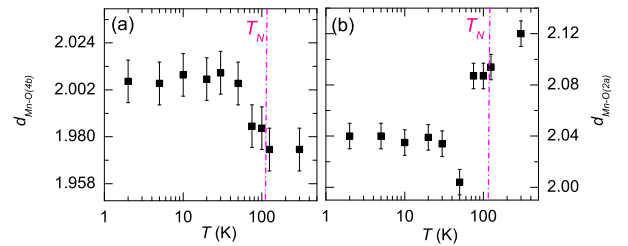


FIG. 4: (colour online) The refined bond lengths (Mn/Fe)-O(4b) and (Mn/Fe)-O(2a) for $\text{LuFe}_{0.5}\text{Mn}_{0.5}\text{O}_3$ are presented in (a) and (b) respectively. The anomalies present in Fig 3 are reflected in the bond distances as well, especially close to T_N , marked by a vertical dotted line.

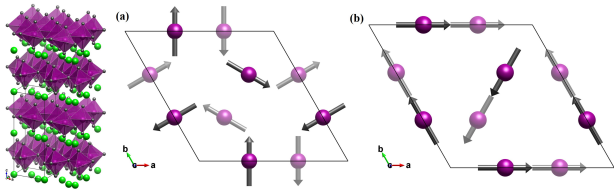


FIG. 5: (colour online) (Left:) A schematic of the hexagonal crystal structure of $\text{LuFe}_{0.5}\text{Mn}_{0.5}\text{O}_3$ at room temperature in the $P6_3cm$ symmetry. The Lu atoms are shown in green, the oxygen atoms in grey and the MnO_5 polyhedra in violet. The unit cell is outlined using a solid line. (Middle, Right:) The possible magnetic arrangements of Mn spins in $\text{LuFe}_{0.5}\text{Mn}_{0.5}\text{O}_3$ viz., (a) Γ_1 ($P6_3cm$) and (b) Γ_3 ($P6'_3cm'$). Only Γ_1 ($P6_3cm$) structure permits magneto-electric coupling. Both the figures were prepared using VESTA[27].

our work is the observation of giant atomic displacements across the magnetic transition thereby suggesting strong spin-lattice coupling. In order to confirm the effects of atomic displacements that is observed in $\text{LuFe}_{0.5}\text{Mn}_{0.5}\text{O}_3$ as presented in Fig 3, the bond distances (Mn/Fe)-O were evaluated from Rietveld refinement results. The Mn/Fe-O($4b$) and Mn-O($2a$) bond distances which are in the basal plane of the hexagonal structure and presented in Fig 4 (a) and (b)

respectively. It is hence clear that the atomic displacements also reflect in the bond distances and is inherent. A schematic of the crystal structure of $\text{LuFe}_{0.5}\text{Mn}_{0.5}\text{O}_3$ in $P6_3cm$ space group is presented in Fig 5 along with Γ_1 and Γ_3 structures.

The magnetic properties of the hexagonal manganite $\text{LuFe}_{0.5}\text{Mn}_{0.5}\text{O}_3$ are studied in this paper using magnetic measurements and neutron powder diffraction. Frustration effects and, importantly, strong spin-lattice coupling are revealed as a result. It is found that the magnetic structure changes from Γ_4 for $h\text{LuMnO}_3$ to Γ_1 representation for $\text{LuFe}_{0.5}\text{Mn}_{0.5}\text{O}_3$ while the nuclear structure remains in $P6_3cm$ space group. By perturbing the Mn lattice in the ab plane through substitution of Fe, the temperature of magnetic ordering is enhanced. The atomic positions undergo significant displacements, especially close to T_N and T_{SR} thereby suggesting strong spin-lattice coupling. Our work attains significance following the recent discovery of room temperature multiferroicity in thin films of $h\text{LuFeO}_3$.

AMS thanks the SA-NRF (93549) and the FRC/URC of UJ for financial assistance. HSN acknowledges FRC/URC for a postdoctoral fellowship. HSN wishes to thank Yixi Su for suggesting this compound.

-
- [1] T. Lottermoser, T. Lonkai, U. Amann, D. Hohlwein, J. Ihringer, and M. Fiebig, *Nature* **430**, 541 (2004).
- [2] S. Lee, A. Pirogov, M. Kang, K. H. Jang, M. Yonemura, T. Kamiyama, S. W. Cheong, F. Gozzo, N. Shin, H. Kimura, et al., *Nature* **451**, 805 (2008).
- [3] B. B. van Aken, T. T. M. Palstra, A. Filippetti, and N. A. Spaldin, *Nat. Mater.* **3**, 164 (2004).
- [4] T. Katsufuji, S. Mori, M. Masaki, Y. Moritomo, N. Yamamoto, and H. Takagi, *Phys. Rev. B* **64**, 104419 (2001).
- [5] B. Lorenz, A. P. Litvinchuk, M. M. Gospodinov, and C. W. Chu, *Phys. Rev. Lett.* **92**, 087204 (2004).
- [6] H. S. Nair, C. M. N. Kumar, H. L. Bhat, S. Elizabeth, and T. Brückel, *Phys. Rev. B* **83**, 104424 (2011).
- [7] S. M. Griffin, M. Lilienblum, K. T. Delaney, Y. Kumagai, M. Fiebig, and N. A. Spaldin, *Phys. Rev. X* **2**, 041022 (2012).
- [8] M. Fiebig, T. Lottermoser, D. Fröhlich, A. V. Goltsev, and R. V. Pisarev, *Nature* **419**, 818 (2002).
- [9] P. J. Brown and T. Chatterji, *J. Phys.: Condens. Matter* **18**, 10085 (2006).
- [10] J. Park, J. Park, G. Jeon, H. Choi, C. Lee, W. Jo, R. Bewley, K. McEwen, and T. Perring, *Phys. Rev. B* **68**, 104426 (2003).
- [11] M. Fiebig, D. Fröhlich, K. Kohn, T. Lottermoser, V. V. Pavlov, R. V. Pisarev, et al., *Phys. Rev. Lett.* **84**, 5620 (2000).
- [12] X. Fabreges, S. Petit, I. Mirebeau, S. Pailhes, L. Pinsard, A. Forget, M. T. Fernandez-Diaz, and F. Porcher, *Phys. Rev. Lett.* **103**, 067204 (2009).
- [13] A. Munoz, J. A. Alonso, M. J. Martinez-Lope, M. T. Casais, J. L. Martinez, and M. T. Fernandez-Diaz, *Phys. Rev. B* **62**, 9498 (2000).
- [14] I. V. Solovyev, M. V. Valentyuk, and V. V. Mazurenko, *Phys. Rev. B* **86**, 054407 (2012).
- [15] H. Das, A. L. Wysocki, Y. Geng, W. Wu, and C. J. Fennie, *Nature Commun.* **5** (2014).
- [16] H. Wang, I. V. Solovyev, W. Wang, X. Wang, P. J. Ryan, D. J. Keavney, J. W. Kim, T. Z. Ward, L. Zhu, J. Shen, et al., *Phys. Rev. B* **90**, 014436 (2014).
- [17] W. Wang, J. Zhao, W. Wang, Z. Gai, N. Balke, M. Chi, H. N. Lee, W. Tian, L. Zhu, X. Cheng, et al., *Phys. Rev. Lett.* **110**, 237601 (2013).
- [18] S. M. Disseler, J. A. Borchers, C. M. Brooks, J. A. Mundy, J. A. Moyer, D. A. Hillsberry, E. L. Thies, D. A. Tenne, J. Heron, J. D. Clarkson, et al., arXiv:1411.1694 (2014).
- [19] P. Fischer, G. Frey, M. Koch, M. Könncke, V. Pomjakushin, J. Schefer, R. Thut, N. Schlumpf, R. Bürge, U. Greuter, et al., *Physica B* **276**, 146 (2000).
- [20] H. M. Rietveld, *J. Appl. Cryst.* **2**, 65 (1969).
- [21] J. Rodriguez-Carvajal, *Physica B* **192**, 55 (1993).
- [22] A. S. Wills, *Physica B* **276**, 680 (2000).
- [23] A. P. Ramirez, Ed. K. H. J. Buschow, Elsevier, Amsterdam **13**, 423 (2001).
- [24] J. Park, S. Lee, M. Kang, K. Jang, C. Lee, S. V. Streltsov, V. V. Mazurenko, M. V. Valentyuk, J. E. Medvedeva, T. Kamiyama, et al., *Phys. Rev. B* **82**, 054428 (2010).
- [25] S. Namdeo, S. S. Rao, S. D. Kaushik, V. Siruguri, and A. M. Awasthi, *J. Appl. Phys.* **116**, 024105 (2014).
- [26] R. W. G. Wyckoff, *Crystal structures vol. 2* (1986).
- [27] K. Momma and F. Izumi, *J. Appl. Cryst.* **44**, 1272 (2011).
- [28] S. M. Disseler, X. Luo, Y. S. Oh, R. Hu, D. Quintana, A. Zhang, J. W. Lynn, S. W. Cheong, I. I. Ratcliff, et al., arXiv:1406.7793 (2014).